DOI: 10.4408/IJEGE.2011-03.B-046

SIMULATION BASED ON FINITE VOLUME METHOD OF THE ENTRAIMENT OF DEBRIS FLOW

YUNYUN FAN(*), SIJING WANG(**), ENZHI WANG(**) & ZHONGGANG LIU(**)

(*) Northeastern University-China - College of Resources and Civil Engineering; email: fyun1982@gmail.com
(**) Tsinghua University-China, State Key laboratory of Hydroscience and Engineering

ABSTRACT

The mountain hazards like snow avalanches, landslides, rock falls, debris flows all have strong destructive power which seriously threaten human lives and belongings. Therefore, it is necessary to study more about the happenings and developments of these disasters. Among the important and common features of the debris flow, the entrainment is the one that can increase the volume of debris flow and affects significantly the flow motion. These influences usually result in a more harmful and stronger destructive power. With the method of finite volume discretization, the numerical simulation of the entrainment process of debris flow is achieved in this paper. The influences of entrainment capabilities on the motion and deposition of debris flow are mainly studied. The typical engineering examples show and prove the stability and effectivity of numerical methods.

***KEY WORDS**: debris flow, entrainment, finite volume, dynamic, simulation*

INTRODUCTION

The dynamic simulation of debris flow can not only improve human cognition in the regularity and characteristics of disasters by inversing and reappearing the development law of debris flow disasters, but also predict the disaster-caused area and intensity of debris flow, and consequently, scientific references of industry planning and construction, and the measures of prevention and reduction of disasters can be offered. Therefore, the dynamic simulation of debris flow is significant and valuable.

In the development of debris flow, the surface bulk material along the way would have a shear failure and slide with debris flow during the motion process so that the entrainment is formed which increase the volume of debris flow and change the composition of motion material. For this reason, the surface material is an important factor in the development of debris flow and should be considered in its dynamic simulation. At the moment, many scholars have begun their studies on the entrainment problems during the motion of debris flow and some progress has been made.

In order to realize the dynamic simulation of debris flow entrainment and study the influences of this entrainment on dynamic simulation, the back analysis is made to study a typical historical debris flow, Nomash River in Canada, by combining entrainment dynamic model theory which considers the entrainment effects and the method of finite volume discretization based on the approximate Riemann solver of HLL Scheme. The calculation also takes the variation of terrain slope caused by entrainment into account. The calculation results which are identical to actual disaster-caused area confirm the effectivity of the dynamic model theory and the numerical solution. Compared with the results which have no consideration of entrainment, the influence of entrainment action on dynamic process of debris flow is analysed.

DYNAMIC MODEL THEORY

BASIC EQUATION

Assuming that the density of debris flow is invariable during the motion process and ignoring the variation of physical variable in the direction of flow depth, the dynamic model equation is as follows:

$$\frac{\partial U}{\partial t}+\frac{\partial E(U)}{\partial x}+\frac{\partial H(U)}{\partial y}=S \tag{1}$$

Where U is conservation variable, F=(E,H) is calculation flux, S is source item, these items can be expressed as follows:

$$E=\begin{pmatrix} hu \\ hu^2+k_{\text{act/pass}}gh^2/2 \\ huv \end{pmatrix}, H=\begin{pmatrix} hv \\ huv \\ hv^2+k_{\text{act/pass}}gh^2/2 \end{pmatrix}$$

$$U=\begin{pmatrix} h \\ hu \\ hv \end{pmatrix}, S=\begin{pmatrix} E_t \\ -gh\partial z_b/\partial x+S_{fx} \\ -gh\partial z_b/\partial y+S_{fy} \end{pmatrix} \tag{2}$$

In this expression, H is the depth of flow, u and v are respectively the velocities in x direction and y direction, g is acceleration of gravity, E_t is the source item of entrainment velocity, z_b is elevation on bottom surface in the coordinate system, and S_f is the source item of resistance, they can be used according to different conditions, $k_{act/pass}$ is the coefficient of lateral stress which can be expressed as (Savage & Hutter, 1989; Iverson & Denlinger, 2001; Pirulli *et alii*, 2007):

$$\frac{k_{\text{act}}}{k_{\text{pass}}}=\frac{2}{\cos^2\varphi}\left(1\mp\sqrt{1-\frac{\cos^2\varphi}{\cos^2\delta}}\right)-1 \tag{3}$$

where φ is internal friction angle and δ is bottom friction angle. Different motion states correspond with different cofficients of lateral stress. When $\partial u/\partial x+\partial v/\partial y>0$, the motion is in active state, however when $\partial u/\partial x+\partial v/\partial y<0$, the motion is in passive state (Savage & Hutter, 1989; Iverson & Denlinger, 2001; Pirulli *et alii*, 2007).

RESISTANCE MODEL

Choosing a correct resistance model of the model equation of dynamic theory is an important step in the dynamic simulation of debris flow. In this paper, analysis is achieved by use of friction resistance and Voellmy resistance.

(1) Friction resistance

During the process of debris flow, the resistance is mainly from the bottom friction, and the friction resistance can be considered as (Savage & Hutter, 1989; Iverson & Denlinger, 2001; McDougall & Hungr, 2005; Pirulli *et alii*, 2007; Hungr, 2009):

$$S_{fx}=-\frac{u}{|\mathbf{v}|}\rho hg\tan\delta \ , \ S_{fy}=-\frac{v}{|\mathbf{v}|}\rho hg\tan\delta \tag{4}$$

where v=(u,v) is velocity vector.

(2) Voellmy resistance

If there exists water during the motion process of debris flow, its resistance effect should also be considered, in this case, Voellmy resistance is usually used as the resistance model (Hungr & Evans, 2004; McDougall & Hungr, 2005; Hungr 2009):

$$S_{fx}=-\frac{u}{|\mathbf{v}|}f\rho hg-\text{sgn}(u)\frac{\rho gu^2}{\xi}$$
$$S_{fy}=-\frac{v}{|\mathbf{v}|}f\rho hg-\text{sgn}(v)\frac{\rho gv^2}{\xi} \tag{5}$$

where sgn(a) is sign function which can be described as:

$$\text{sgn}(a)=\begin{cases} 1 & a>0 \\ 0 & ,a=0 \\ -1 & a<0 \end{cases} \tag{6}$$

In eq. (5), f is friction coefficient, ξ is hydraulic parameter, the first item from the right hand represents friction resistance which has the same form with eq. (4), f corresponds to tan δ, and the second item represents other resistances, which are experientially used to express the items relative to velocity in the analysis.

ENTRAINMENT VELOCITY

The entrainment velocity form of Hungr is used in this paper (Hungr & Evans, 2004; McDougall & Hungr, 2005), so the relationship between entrainment velocity E_t and rate of increase of entrainment E_s is as follows:

$$E_t=E_s h|\mathbf{v}| \tag{7}$$

A reasonable E_s can be obtained only if it is ajusted according to the actual condition repeatedly. One feasible method is to use the average rate of increase $\bar{E}_s$, obtained by use of the total volume before and after entrainment, which can be describes as:

$$\bar{E}_s=\frac{\ln(V_f/V_0)}{\bar{d}} \tag{8}$$

where V_0 is the total volume before entrainment, and V_f after entrainment, and $\bar{d}$ is the approximate average length in entrainment area.

FINITE VOLUME NUMERICAL METHOD

FINITE VOLUME DISCRETIZATION

The computational domain is discretized by using the layout form of the triangle unstructured triangular meshes and Cell Center which have a great adaptability.

Changing eq. (1) into vector form, then find the integral of this vector form:

$$\int_{V_i}\frac{\partial U}{\partial t}dV+\int_{V_i}\nabla\cdot FdV=\int_{V_i}SdV \tag{9}$$

Considering the U_i and S_i as the average values of element variable and source item respectively, and placing them in the centre of element, then:

$$U_i=\frac{1}{A_i}\int_{V_i}UdV_i \ , \ S_i=\frac{1}{A_i}\int_{V_i}SdV \tag{10}$$

By using the Green formula to transform eq. (9) from surface integral to line integral, it is obtained that:

$$\frac{\Delta U_i}{\Delta t}A_i+\oint_L F\cdot ndl=S_iA_i \tag{11}$$

where L is the boundary of the ith element, A_i is the surface of element i, $n=(n_x,n_y)=(\cos\theta,\sin\theta)$ is the direction of exterior normal, and θ is the angle between the exterior normal and x-axis.

The following equation can be obtained by discretizing eq. (11):

$$\Delta U_i=-\frac{\Delta t}{A_i}\sum_{j=1}^{3}(F_{ij})\Delta l_{ij}+\Delta tS_i \tag{12}$$

where ΔU_i is the increment of variable, Δl_{ij} is the side length of element, F_{ij} represents the normal numerical flux at the j th edge of the i th element.

NUMERICAL FLUX CALCULATION

The present model employs the HLL Riemann solver to compute the normal flux at the face of an element as follows (Harten *et alii*, 1983; Aliparast, 2009):

$$\mathrm{F}^*\cdot n=\begin{cases}F_L\cdot n & s_L\ge 0\\ \dfrac{s_RF_L\cdot n-s_LF_R\cdot n+s_Rs_L[(U_R)-(U_L)]}{(s_R-s_L)} & s_L<0<s_R\\ F_R\cdot n & s_R\le 0\end{cases} \tag{13}$$

where L and R are variables at the inner edge and outer edge respectively; $(U_L)_{i,j}$ and $(U_R)_{i,j}$ are the U value on the left and right sides at the j th edge of the i element, respectively; s_L and s_R are wave velocities of the both edges, respectively, it can be expressed that:

$$\begin{aligned}s_L&=\min(u_Ln_x+v_Ln_y-c_L,u^*-c^*)\\ s_R&=\max(u_Rn_x+v_Rn_y+c_R,u^*+c^*)\end{aligned} \tag{14}$$

where , $c=\sqrt{k_{\text{act/pass}}gh^2/2}$ u^* and c^* can be described as follows:

$$\begin{aligned}u^*&=\frac{(u_L+u_R)n_x+(v_L+v_R)n_y}{2}+c_L-c_R\\ c^*&=\frac{c_L+c_R}{2}+\frac{(u_L-u_R)n_x+(v_L-v_R)n_y}{4}\end{aligned} \tag{15}$$

when the left side is dry, s_L and s_R can be calculated as follows:

$$\begin{aligned}s_L&=u_Rn_x+v_Rn_y-2c_R\\ s_R&=u_Rn_x+v_Rn_y+c_R,(h_L=0)\end{aligned} \tag{16}$$

when the right side is dry, s_L and s_R can be calculated as follows:

$$\begin{aligned}s_L&=u_Ln_x+v_Ln_y-c_L\\ s_R&=u_Ln_x+v_Ln_y+2c_L,(h_R=0)\end{aligned} \tag{17}$$

SPATIAL SECOND-ORDER LINEAR RECONSTRUCTION

When the numerical discretization method of finite volume is employed, the variable of the control volume of spatial second-order accuracy should be distributed linearly. With the MUSCL method (Osher, 1996), the states of the both edges are concluded by interpolating variables, the linear reconstruction on unstructured mesh is as described in Fig.1.

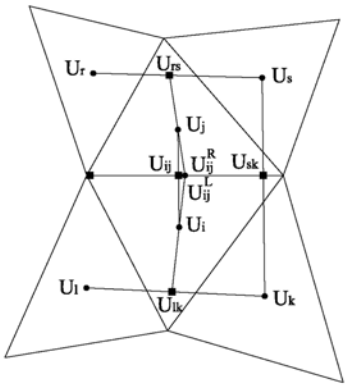

Fig. 1 - Schematic plan of numerical reconstruction

In Fig. 1, U_i, U_k, U_l, U_j, U_s and U_r are centroid values of the element, U_{lk}, U_{lr}, U_{ij}, U_{ks}, and U_{rs} are linear interpolation, while U^L_{ij} and U^R_{ij} are the linear upwind values at the both edges, obtained by extrapolating variables, U^C_{ij} is the central value at the edge.

The limited linear interpolation values are used to calculated the variables at the both edges:

$$\begin{aligned}(U_L)_{ij}&=U_i+\Phi(r^l_{ij})(U^L_{ij}-U_i)\\ (U_R)_{ij}&=U_j+\Phi(r^r_{ij})(U^R_{ij}-U_j)\end{aligned} \tag{18}$$

where the slope of linear interpolation can be expressed as:

$$r^l_{ij}=\frac{U^C_{ij}-U_i}{U^L_{ij}-U_i} \ , \ r^r_{ij}=\frac{U^C_{ij}-U_j}{U^R_{ij}-U_j} \tag{19}$$

In order to make the scheme satisfy the needs of TVD, $\Phi(r)$ employs the scheme of Van leer:

$$\Phi(r)=\frac{r+|r|}{1+\max(1,|r|)} \tag{20}$$

Besides, with Runge-Kutta methods (Hubbard *et alii*, 1999), the format of space-time second order accuracy is obtained.

CALCULATION OF TERRAIN SLOPE

Among the source items, the derivative term of elevation on bottom surface should be especially traited. On unstructured triangular meshes, through the calculation with the coordinate values of the three nodes of the triangle element, this derivative term can be obtained as follows:

$$\begin{aligned}\frac{\partial z_b}{\partial x} &= \frac{1}{2A_i}(z_{b1}(y_2-y_3)+z_{b2}(y_3-y_1)+z_{b3}(y_1-y_2))\\ \frac{\partial z_b}{\partial y} &= \frac{1}{2A_i}(z_{b1}(x_3-x_2)+z_{b2}(x_1-x_3)+z_{b3}(x_2-x_1))\end{aligned} \quad (21)$$

where (x_k, y_k) represents the coordinate value of the k th node of the i th triangle, z_{bk} represents the elevation on bottom surface of the k th node in the coordinate system.

During the process of entrainment, elevation on bottom surface changes with the reduction of the bottom mass, at this time, the elevation on bottom surface reconstructs linearly in space like other variables above-mentioned, so the derivative term of the source items can be calculated with the reconstructed values of the element:

$$\begin{aligned}\frac{\partial z_b}{\partial x} &= \frac{2}{A_i}(z_{bL1}(y_{i2}-y_{i3})+z_{bL2}(y_{i3}-y_{i1})+z_{bL3}(y_{i1}-y_{i2}))\\ \frac{\partial z_b}{\partial y} &= \frac{2}{A_i}(z_{bL1}(x_{i3}-x_{i2})+z_{bL2}(x_{i1}-x_{i3})+z_{bL3}(x_{i2}-x_{i1}))\end{aligned} \quad (22)$$

where (x_{ij}, y_{ij}) represents the coordinate value of the middle point of the j th edge of the i th triangle element, z_{bLj} represents the internal elevation of bottom surface of the j th edge which is obtained through the spatial second-order linear reconstruction.

CALCULATION AND ANALYSIS OF AN EXAMPLE

NOMASH RIVER DEBRIS FLOW

Nomash River lies in the west part of British Columbia, Canada, the area bedrock is mainly made of crystalline limestone.

In April 1999, a debris flow occurred in the upper course of the Nomash River during spring snowmelt, as shown in Fig. 2. The source area located on a mountain slope angled at 50° to the northeast of the U-shaped river valley. At the beginning, a continuous shear plane was formed after a series of crossed joints about 430 m above the river, then 300 000 m^3 of crystalline limestone was seperated and suddenly collapsed. Assuming 25% bulking of the source failure, there was 375.000 m^3 of fragments produced by the slide, which fell into the valley of the Nomash River perpendicularly (Hungr & Evans, 2004; McDougal & Hungr, 2005).

Fig. 2 - Nomash River debris flow

Fig. 3 - Entrainment area of Nomash River debris flow

Before reaching the valley bottom, an additional 360 000 m^3 of saturated colluvium was impacte by the entraiment, and the entrainment ration reached 0.96 which is really alarming number. After the entrainment, a 100~150 m-wide erosion area was left, the vestige and trace of entrainment are visible in Fig. 3

CALCULATION AND RESULT ANALYSIS

The topographic condition used in back analysis is from the results of Hungr and Evans (McDougall & Hungr, 2005), by modifying the topography after the debris flow. The volume before and after the entrainment is V_0=375.000 m^3 V_f=735.000 m^3 and respectively, the average length of the erosion area is $\bar{d}$=350 m, and according to eq. (8), $\bar{E}_s$=0.0019 m^{-1} is obtained; before the entrainment, the friction resistance model is employed, where the internal friction angle φ=35°, and the bottom friction angle δ=30°, when the entrainment happened, Voellmy

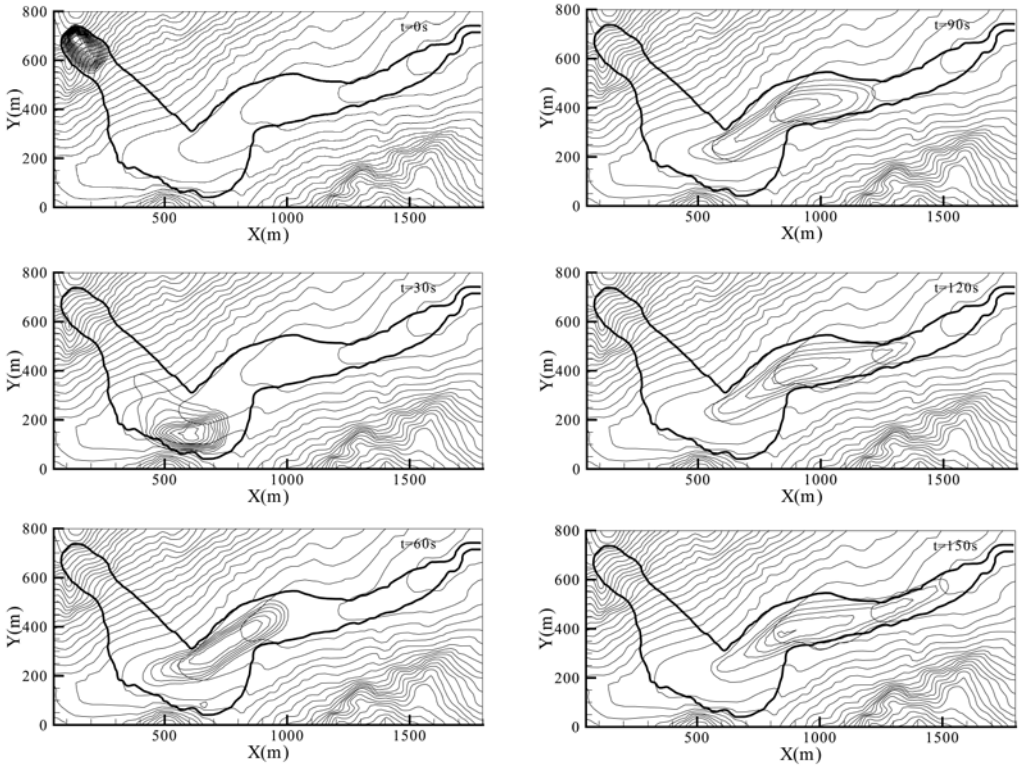

Fig. 4 - Calculation results at different times

resistance model is used, and the calculation parameters are ξ=400 m/s^2 and f=0.05. With the above method, the results at different time are obtained as shown in Fig.4.

It can be seen from Fig.4 that the thick real line represents the real disaster-caused area, the interval between the geography contours is 20m, and the flow depth contour is 1m. It can be seen from the above calculation that the back analysis shows the whole motion process of the debris flow: at the 30th s, the flow motion after the entrainment almost arrived at the highest point of the opposite mountain slope, at the 60th s, the flow motion went backward after a second turning, and the deposit was gradually formed. Certes, there still exists some differences between the calculation results and actual situation, and the calculation results could be more exact if a more reasonable modification of geography can be made and the calculation parameters of entrainment of path material which can better conform to the actual situation are applicable. Nevertheless, it is still satisfactory that the simulation results are relatively identical to actual disaster-caused area.

It can be seen from the calculation that the entrainment effect which greatly increases the motion volume is very significant in the dynamic process of debris flow. The final results in Fig.5 obtained at the 40th second are calculated without considering entrainment effects.

The above results show that without regard to entrainment, the deposit will stop at the valley bottom because of lacking forces which can push it to climb the slope, as a result, the disaster-caused area is much smaller than that is shown in Fig.4. Thus it is known that entrainment plays a very important role during a dynamic process of debris flow. It makes debris flow more powerful and harmful and should be considered as a key factor in the formation of large-scale debris flows.

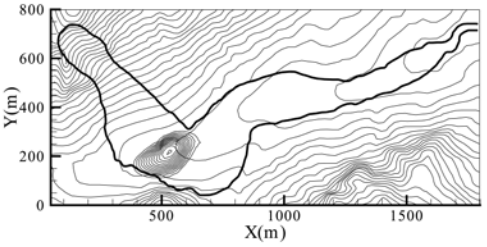

Fig. 5 - Calculation results without the consideration of entrainment

CONCLUSIONS

Entrainment is one of the most important factors that can not be ignored in the dynamic process of debris flow, which should be considered in the dynamic simulation of debris flows.

The dynamic simulation of the entrainment of debris flow is realized by combining entrainment dynamic model theory and the method of finite volume discretization. The variation of terrain slope caused by entrainment is also considered in the simulation. The back analysis is made to study Nomash River debris flow, a typical historical debris flow happened in Canada. The calculation results which are relatively identical to actual disaster-caused area confirm the effectivity of the dynamic model theory and the numerical solution. Compared with the results which have no consideration of entrainment, it is can be seen that the entrainment action can increase the motion volume of entrainment, change the composition of motion materials and enhance the motility of debris flow, so that the entrainment will be more destructive and harmful. In fact, entrainment is a main cause of large-scale debris flow, so it should be paid more attention in the dynamic simulation of debris flow.

REFERENCES

Aliparast M. (2009) - *Two-dimensional finite volume method for dam-break flow simulation*. International Journal of Sediment Research, **23** (**1**): 99-107.

Harten A., Lax P.D. & Vanleer B. (1983) - *On upstream differencing and Godunov-type schemes for hyperbolic conservation laws*. SIAM Review, **25** (**1**): 35-61.

Hubbard M.E. (1999) - *Multidimensional slope limiters for MUSCL type finite volume schemes on unstructured grids*. Journal of Computational Physics, **155** (**1**): 54-74.

Hungr O. & Evans S.G. (2004) - *Entrainment of debris in rock avalanches; an analysis of a long run-out mechanism*. Geological Society of America Bulletin, **116** (**9**/**10**): 1240–1252.

Hungr O. (2009) - *Numerical modelling of the motion of rapid flow-like landslides for hazard assessment*. Ksce Journal of Civil Engineering, **13** (**4**): 281-287.

Iverson R.M. & Denlinger R.P. (2001) - *Flow of variably fluidized granular masses across three-dimensional terrain: 1 Coulomb mixture theory*. Journal of Geophysical Research, **106** (**B1**): 537-552.

McDougall S. & Hungr O. (2005) - *Dynamic modelling of entrainment in rapid landslides.* Canadian Geotechnical Journal, **42** (**5**): 1437-1447.

Osher S. (1996) - *Convergence of generalized MUSCL schemes*. SIAM Journal of Numerical Analysis, **22** (**5**): 947-961.

Pirulli M., Bristeau M.O. & Mangeney A. (2007) - *The effect of the earth pressure coefficients on the runout of granular material*. Environmental Modelling & Software, **22** (**10**): 1437-1454.

Savage S.B. & Hutter K. (1989) - *The motion of a finite mass of granular material down a rough incline*. Journal of Fluid Mechanics, **199**: 177-215.